Romain Mesnil, Takara Muto, Krittika Walia, Cyril Douthe, Olivier Baverel

Design and Fabrication of a Pseudo-Geodesic Gridshell

Abstract: The aim of this paper is to present the design and construction of a GFRP gridshell based on pseudo-geodesic curves. Pseudo-geodesic curves on a surface have a constant angle between their normal vector and the surface normal. They are thus a generalization of asymptotic curves (where this angle is equal to 90°) or geodesic curves (where this angle is 0° or 180°), which have already been used to construct elastic gridshells. Like asymptotic or geodesic gridshells, pseudo-geodesic gridshells benefit from a flat unrolling property as well as a standard connection detail. The paper presents the design strategy of the first pseudo-geodesic gridshell. A parametric structural analysis shows that the gridshell outperforms geodesic gridshells significantly but also that it is sensitive to local lateral-torsional buckling. The fabrication stage confirmed that the construction of a unique type of connector is possible. In total, 160 connectors have been used for the prototype. The mathematical properties of pseudo-geodesic curves have thus been successfully turned into a technological solution to materialize doubly curved shapes.

1 Introduction

1.1 Context

Gridshell structures are efficient structural systems that enclose large volumes with little material. The rationalization of their construction is an active topic of research in the architectural geometry community, as it is deeply related to the fundamental properties of discrete networks and to the mechanical behavior of the structure. This article studies *elastic gridshells,* which are constructed through the elastic deformation of slender beams. Case studies have shown that a significant share of cost and engineering is spent on node design [1]. Following recent research on fabrication-aware design, we are thus interested in the design of a gridshell with *congruent nodes* [2,3].

1.2 Previous Work

Some gridshells were built with circular hollow sections and swivel connectors, following Frei Otto's experiments with rebars [4]. However, most elastic gridshells are built with anisotropic cross-sections, like planks. Two factors may explain this: first,

https://doi.org/10.1515/9783111162683-007

Fig. 1: Two gridshells with high node congruence and straight development: the Polydome at EPFL (left) and the Inside/Out Pavilion at TU Munich (middle) and the pseudo-geodesic gridshell (right).

connections between planks are easier to construct, and second, materials adapted to the materialization of gridshell structures are usually fibrous materials, like timber or GFRP, and can easily be produced as planks [5]. Two rationalization strategies have been proposed to guarantee two properties: *node repetition* and *straight-flattening*.

Julius Natterer proposed to build geodesic gridshells, where planks are laid along geodesic curves of the reference surface [6]. The *Polydome* at EPFL is a fine example of this approach. Schling et al. [2] later proposed to construct asymptotic gridshells, where the planks are laid perpendicular to the surface osculating plane. Asymptotic gridshells are limited to negative curvature, and Schling proposed to construct them with planks that have an initial geodesic curvature. The main drawback of this approach for fiber-reinforced materials is that the material anisotropy is disregarded, and remains limited to isotropic materials, like steel.

An extension of the two design approaches has been proposed with pseudo-geodesic gridshells [8]. The authors claim that this structural system improves structural efficiency compared to geodesic gridshells while offering more formal possibilities than asymptotic gridshells. However, no experimental validation has been made yet.

1.3 Problem Statement

Asymptotic and geodesic gridshells are well-known structural systems that allow cost-effective materialization of doubly curved shapes. However, both systems have practical limitations: either the need for a double layer or strong formal constraints. Pseudo-geodesic gridshells offer the potential to find a compromise between the two approaches. The geometrical properties of pseudo-geodesic curves seem to allow for the construction of nodes with high congruence.

The aim of this paper is to discuss the potential application of pseudo-geodesic gridshells through a practical case study. We first present some theoretical considerations on pseudo-geodesic gridshells and highlight their potential for the construction of efficient structures. We then discuss the design of the *Pseudo-Geodesic Pavilion*, with critical feedback on the design tools currently available. We conclude the paper by

presenting the construction of the pavilion, with a special focus on constructive details and their link to geometry.

2 Pseudo-Geodesic Gridshells

2.1 On Straight Flattening

The straight flattening property is linked to an underlying assumption for the geometry of the strip that requires some comments, since previous publications [2] focus on the geometric formulation of the problem. Here, we consider a thin strip that is to be mapped to an unstressed (generally planar) configuration, as shown in Fig. 2. We adopt a beam model [9,10], where the beam is described by a curve Γ and the ruling direction $\mathbf{r}$ (material frame).

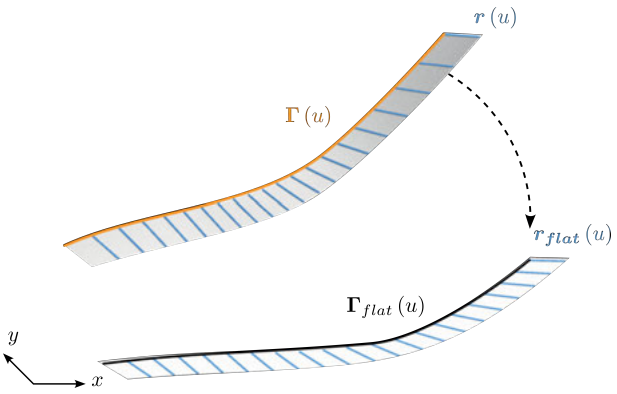

Fig. 2: A possible flattening of a ruled surface.

The strain energy of the strip, with the assumption of inextensibility, is given in Eq. (1):

$$\mathcal{E} = \frac{1}{2}\int_0^L \left[EI_1(\kappa_1 - \overline{\kappa}_1)^2 + EI_2(\kappa_2 - \overline{\kappa}_2)^2\right] ds + \frac{1}{2}\int_0^L GJ(\tau - \overline{\tau})^2 ds \tag{1}$$

where κ_i are curvatures in the material frame and τ is the torsion (with respect to a rotation-minimizing frame on the final configuration). Symbols with overlines correspond to the curvatures and torsions of the unstrained configuration. For an initially straight rod, they are null. The flattening problem consists of minimizing the strain energy with respect to the unstrained curvature and torsion.

When the ruled surface is also developable, it is admitted that the flat unrolling problem has a solution, thanks to *Theorema Egregium*. The computation of isometric

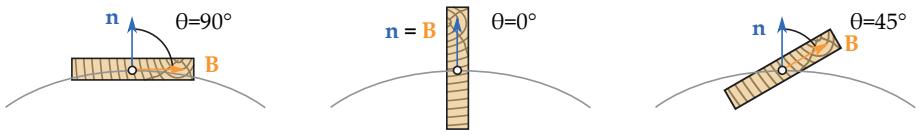

Fig. 3: Orientation of planks for geodesic gridshells (left), asymptotic gridshells (middle), and pseudo-geodesic gridshells (right) [6].

transformations corresponds to an inextensibility constraint, which imposes the torsional strain energy to be zero (the material frame follows the rotation-minimizing frame). It is also admitted that the unrolling is straight and planar when the ruling direction (or material frame) is along the binormal vector **B** of the curve: this is precisely the case for geodesic and asymptotic gridshells. In such cases, it is easy to verify that the strain energy is the sum of bending energy along the weak axis and torsional energy, as detailed in eq. (2):

$$\mathcal{E} = \int_0^L EI_2\kappa^2 ds + \int_0^L GJ\tau^2 ds \tag{2}$$

It is therefore assumed that the contribution of bending along the strong beam axis to the total strain energy is much higher than the two others and that the laths tend to avoid this flexural mode. Indeed, when the ratio between lath height h and width b goes to zero, the bending stiffness along the strong axis $Ehb^3/12$ becomes much larger than the two other stiffnesses $Ebh^3/12$ and $Gbh^3/4$.

2.2 Pseudo-Geodesic Curves

Pseudo-geodesic curves were first studied by Wunderlich [11] and later applied in architectural geometry [7]. They are curves traced on surfaces so that the angle between the curve binormal **B** and the surface normal **n**, written θ is a constant. Another definition is that the ratio between total curvature and normal curvature is constant, thanks to Meusnier's theorem:

$$\frac{\kappa_n}{\kappa} = \sin\theta \tag{3}$$

The ruled surface generated by the envelope of binormal vectors has a straight flattening property. It also has a constant angle with the surface normal. This property can be used to construct congruent connectors. Geodesic and asymptotic curves are special cases of pseudo-geodesic curves with $\theta = 90°$ and $\theta = 0°$ respectively (see Fig. 3).

One of the natural questions that one may ask is whether it is possible to cover a shape with a pseudo-geodesic net. Indeed, it is known that geodesics can be constructed through any point in any direction, while asymptotic curves only exist on anticlastic surfaces. Mesnil and Baverel have constructed a lower bound for the total curvature of

pseudo-geodesic curves on synclastic surfaces by combining the Meusnier theorem and Euler's formula, recalled in eq. (4).

$$|\kappa| > \frac{|\kappa_2|}{\sin\theta} \tag{4}$$

This equation has practical implications for the construction of elastic gridshells since the bending stress in the laths is proportional to curvature and should remain below the design stress, as shown in eq. (5):

$$\sigma_{\max} = \frac{E\kappa h}{2} < \sigma_d \tag{5}$$

Therefore, the inequality constraint from eq. (4) becomes an inequality on the strip height h:

$$h < \frac{2\sigma_d \sin\theta}{E|\kappa_2|} \tag{6}$$

In practice, laths with high curvature have to be thinner, reducing the stiffness of the structure.

2.3 Mechanical Performance

Mechanical efficiency was one of Frei Otto's main motivations for constructing elastic gridshells. The construction of safe structures with as little material as possible is still highly relevant in the current context of dwindling resources and climate change. Pseudo-geodesic gridshells offer a compromise between geodesic and asymptotic gridshells and may mitigate some of their limitations.

First, we shall recall that gridshells are efficient because of their ability to transfer out-of-plane loads through axial forces in their members. This is only possible when the curves have *normal* curvature. Thus, asymptotic gridshells mainly work through bending because asymptotic curves have no normal curvature. This fact was hinted at by Panozzo and coauthors [15], who noticed that the orientation of thrust networks in negatively curved regions is severely constrained. In contrast, geodesic curves only have normal curvature, and are therefore more likely to work as a true gridshells.

Second, gridshells are known to be prone to buckling, which depends on their bending stiffness. A homogenized bending stiffness D has been proposed in [6] based on prior works:

$$D \sim \frac{E}{l}\left(\frac{hb^3}{12}\cos^2\theta + \frac{bh^3}{12}\sin^2\theta\right) \tag{7}$$

When factoring in the restriction on maximal strip height h imposed by eq. (6), it appears that the optimal angle θ is around 45°. However, a parametric study on toroidal caps in [6] shows that pseudo-geodesic gridshells may be sensitive to local lateral-torsional buckling, and that the optimal θ angle was around 30°.

3 Designing the Pseudo-Geodesic Pavilion

A full-scale pseudo-geodesic gridshell was constructed as a pavilion to investigate the feasibility of the concept (see Fig. 4). This section discusses practical design issues and strategies employed to materialize the pseudo-geodesic pavilion.

Fig. 4: The pseudo-geodesic pavilion, made of 100 mm GFRP lath at 60° with a unique Z-connector. (Picture: Charlene Yves)

3.1 Design Constraints

The pavilion spans a rectangular frame. Covering a fixed boundary is a common design problem in gridshells; notable examples include the courtyards of the British Museum in London, the Odeon in Munich, or Dresden Castle. The pavilion is covered with polycarbonate panels. The length of the rectangle is $L = 6$ m, while the short span is 4 m. Following [6], we choose an angle of 60°, the best compromise between bending stiffness and flexural torsional buckling.

A CAD-based approach [12,13] was used for the design because several constraints required adjustments for the production of shop drawings. The reference surface is a NURBS with globally positive gaussian curvature but locally negative curvature in the corners of the surface. Several design goals or constraints were at stake:

- Limit the distortion of the mesh, designed to be as uniform as possible;
- Minimize the number of rods while satisfying ULS design criteria, including buckling;
- Maintain planarity of panels within acceptable limits for a cover with thin polycarbonate sheets.

3.2 Grid Generation

Pseudo-geodesics on arbitrary surfaces are usually generated with a shooting method [7,8]. Indeed, once a seed point and a tangent vector have been chosen, a unique pseudo-geodesic curve can be traced (when $\theta \neq 0$). The main limitation with this approach is the difficulty of controlling the behavior of the pseudo-geodesic away from the seed point, as already noticed in [7]. The morphological strategy is represented in Fig. 5: a geodesic splitting the surface in two regions was traced, and tangent vectors along this curve can be generated as a list of scalar values. The second network was generated by symmetry. With this strategy, the parameters controlling the appearance of the grid are the number of points, the orientation of the pseudo-geodesics and the spacing between seed points on the geodesic. Choosing the spacing corresponds to a reparametrization of the curve which is here optimized to get a uniform meshing of the surface (see Fig. 6, 90 cm).

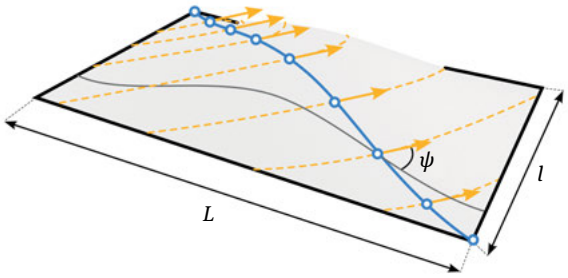

Fig. 5: Generation of the pseudo-geodesic net. A geodesic splitting the surface is chosen (blue). Each tangent vectors (orange) is described by the scalar ψ, which represents the angle between the pseudo-geodesic and the isoparametric curve going through the seed point (blue).

3.3 Shape Variations

A sensitivity study was performed to select the geometry that satisfied construction and mechanical constraints. Figure 6 shows the top view of five different grids. The higher the rise of the surface, the more positive Gaussian curvature there is, and the more irregular the pseudo-geodesic net becomes. The angles φ measuring deviation from perpendicularity for each connector are shown in Tab. 1 (smaller values are preferred). Since pseudo-geodesic curves have a tendency to have more total curvature on positively-curved surfaces, gridshells with lower rises are preferable.

Beyond deviation angles, the planarity of quad panels aligned with the pseudo-geodesic network is also evaluated for the 5 grids (see Tab. 1). It is measured as the ratio between the distance between the two diagonals and the length of the longest diagonal. As expected, the more total curvature in the surface, the larger the planarity

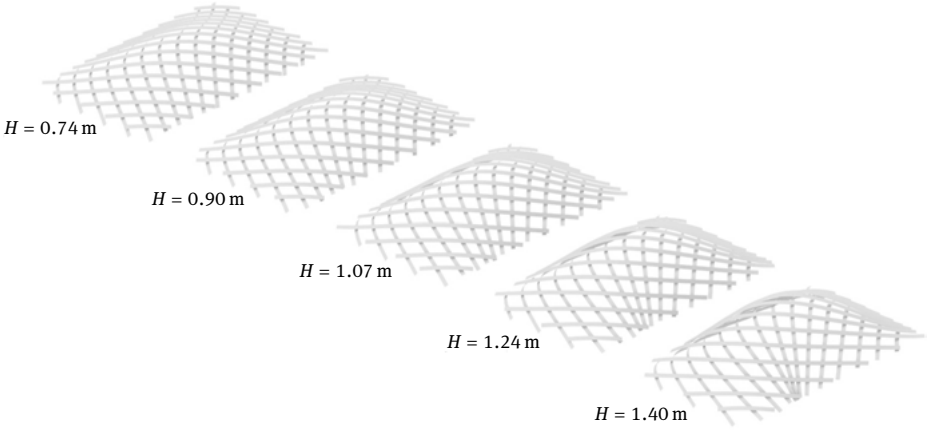

Fig. 6: Perspective view of the pavilion for pseudo-geodesics with $\theta = 60°$. The network becomes irregular for surfaces with a higher rise.

Tab. 1: Comparison of key features of the five grid configurations presented in Fig. 6. The grid with 90 cm height will be finally chosen as a good compromise between mechanical and geometrical constraints.

Gridshell height	74 cm	90 cm	107 cm	124 cm	140 cm
Min. deviation angle φ_{min}	−24°	−29°	−36°	−42°	−46°
Max. deviation angle φ_{max}	17°	19°	20°	24°	32°
Average planarity default	1.2 %	1.6 %	2.1 %	2.6 %	3.0 %
Max. planarity default	3.0 %	4.4 %	6.3 %	8.9 %	12.7 %
Max. lath curvature	0.43 m^{-1}	0.51 m^{-1}	0.59 m^{-1}	0.68 m^{-1}	0.76 m^{-1}
Max. vertical deflection	4.3 mm	4.2 mm	5.6 mm	5.8 mm	8.3 mm

default. For all configurations, the ratio exceeds the usual value accepted for glass panels (0.5 %) with only one quarter of the panels below this threshold.

Concerning mechanical performances, two criteria were selected during this feasibility study. The first one is linked with the prestress level of the laths, which is proportional to the curvature of the lines: the higher the curvature, the higher the permanent bending stresses, and by extension, the lowest the admissible lath thickness. The second one is linked to the grid stiffness, which is here evaluated as the maximum deflection of a grid made of 100 mm wide and 8 mm thick laths under self weight. Both are presented in Tab. 1. For the lath curvature, results follow intuition: values grow with the grid height but remain admissible for all grids (for the laths and material used for the prototype, the maximum allowable curvature is 0.83 m^{-1}). On the contrary, for

the deflection, the highest surfaces show the lowest mechanical performances, which comes from the irregularity of grids on highly curved shapes (see Fig. 6).

The surface with $H = 90$ cm was selected in the end, as a good compromise between fabrication and mechanical constraints. The rise-over-span ratio is 22.5 %, which is still compatible with a pure shell behavior.

3.4 Structural Analysis

The CAD-Based design space exploration allowed the design of a grid structure satisfying SLS and ULS criteria with 30 GFRP laths, with a cross-section of 8 mm × 100 mm. The grid weighs 170 kg and 160 connectors cumulatively weigh 95 kg. The governing factor for design is the buckling: we restricted our study to a linear buckling analysis, and made sure that the buckling factor remained superior to 10, which is arguably a conservative approach. The first buckling mode was a lateral-torsional buckling.

Additionally, sensitivity analysis was conducted: the angle θ was sampled between 50° and 90° and finite element analysis was conducted on each geometry similarly to 6]. Some results are summed up in Fig. 7: first, they confirm Mesnil et al. founding [6]: 60° is the best angle on this surface and the mechanical efficiency of our design is doubled compared to geodesic gridshells. Second, they also show that the pre-stress due to bending (around 130 MPa) is much more than stress induced by external loads (around 15 MPa for critical wind load). Finally, the sensitivity to the addition of a triangulation was also studied: adding a triangulation doubles the stiffness, which is less than for other projects [4]. We explain this by the relatively small scale of the pavilion, by the

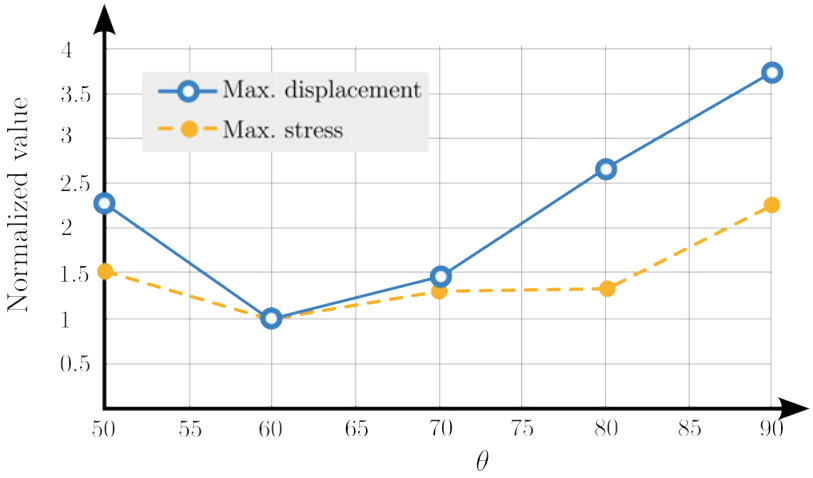

Fig. 7: Relative gridshell performance for various lath inclinations for a uniform load of 1 kPa applied to the structure.

fact that the grid is not a Chebysheff: the inclination of laths makes the in-plane shear stiffness rather high, which limits the need for additional bracing. The sensitivity of pseudo-geodesic gridshells to bracing may be an interesting research direction in the future.

4 Fabrication of the Pseudo-Geodesic Pavilion

4.1 High Node Congruence

One of the main contributions of this case-study is the joint design, which translates some geometrical properties of pseudo-geodesic curves into technological strategies. One of the main objectives was to construct congruent nodes that could be assembled from standard components. Additionally, the intersection of the laths is not allowed like it is done in a scissor joint, as the sensitivity of the composite material to crack or notch, and also to allow the re-usage of the laths after the structure is disassembled. Thus, the connectors are eccentric to the laths. In practice, this means that the neutral axes of the beams are not on the target surface; they are reconstructed from the ruling direction of the pseudo-geodesic strip.

Figure 8 shows a congruent connector satisfying the geometrical requirements. It mainly consists of two stainless steel Z plates and one long bolt passing through its center, allowing rotation in one direction. The Z plate serves to maintain the constant angle between two vectors, which was 60° in our case. The centerline of the laths is offset, and it is clamped between the Z plate and the small plate. Jappy bolts were used, which allowed the laths to be pressed easily at an accurate position. This pressing is essential to transmit shear force. Additionally, EPDM tape was used at the location of the connectors in order to increase the frictional force between the laths and the steel connector.

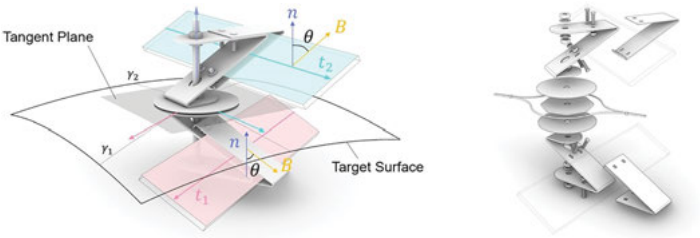

Fig. 8: Alignment of connector with respect to the given surface (left) and exploded view (right).

4.2 Grid Assembly

The network of the shell consists of the initially straight flat laths made of GFRP. Unlike most elastic gridshells, the structure was not deployed but assembled lath by lath. Indeed, the structure does not have repeating lengths. This property may be one of the factors explaining the stiffness of the structure and the relatively low influence of triangulation on the buckling capacity and stiffness of the gridshell. The assembly of all laths was done in one day. The inclination of the laths brings several architectural properties, such as semi-transparency of the roof and a unique edge of the eaves. Hence, the solar shading differs at different angles (see Fig. 9, the lower layer seems much wider than the upper one).

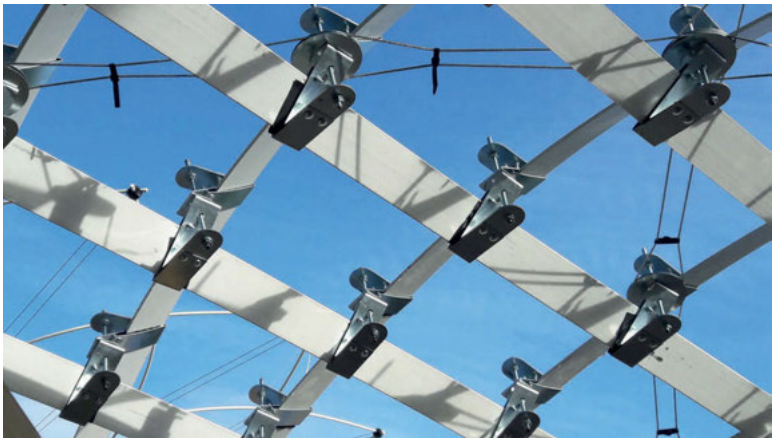

Fig. 9: The standard nodes developed in this study and bracing system. Laths cross-section: 100 × 8 mm.

4.3 Bracing

The circular plates and octagonal plate (Fig. 9) in the middle of the connectors serve as the fixture for a diagonal cable for bracing, allowing triangulation of the existing mesh of the pavilion. Cables were pulled inward thanks to zip ties. The geometry of the bracing, reminiscent of pre-stress strategies invented by Eladio Dieste [14], acts as a mechanical amplifier: a small pinching force results in a large tension in the cable. All the plates of the connector assemble together at one node, which gives semi-transparency to this grid shell.

4.4 Covering

The prototype was finally covered with 3 mm-thick polycarbonate quads aligned with the pseudo-geodesic network. As discussed in Section 3.4, the deviation from planarity is limited, and panels can be easily obtained from a flat sheet of material. Before fabricating the panels, it was decided to control the geometrical accuracy of the grid, whose form was only determined by the position and orientation of the anchorage and connectors. To this end, the length of every edge and diagonal was measured for each quad panel. An average accuracy of ±0.5 % on the diagonal length was found, corresponding to a very acceptable ±3 mm in the positions of the connector axes. As the panels are point-fixed, this accuracy can be easily handled through tolerances in panel openings. An overview of the covered gridshell is presented in Fig. 10: panels rest locally on the top surface of the connectors, which is parallel to the reference surface (see Fig. 8) and use the connector axes for clamping.

Fig. 10: Gridshell covered with quadrangular polycarbonate shingles.

5 Conclusion

This paper investigates the potential of pseudo-geodesic gridshells through the design and fabrication of a composite gridshell. The study confirmed that the straight flattening property can be achieved with high node congruence for pseudo-geodesic gridshells. A parametric study has also shown that the structure outperforms a similar geodesic gridshell on the same surface, confirming previous results [6].

Some questions are left open for future work. Regarding design, the tracing of pseudo-geodesics still relies on a shooting method that is difficult to control. An ad hoc design strategy was developed, but gaining a better understanding of the behavior

of pseudo-geodesic nets would be a great help to designers. Regarding mechanical efficiency, lateral-torsional buckling is the critical failure mode; individual member stabilization is thus a new research topic worthy of exploration. Regarding the covering, a proposition was made using nearly-planar polycarbonate shingles; other solutions could be explored in combination with stabilizing systems against member lateral-torsional buckling. From an architectural point of view, the asymmetry of the grid due to the constant angle of the lath with the surface normal introduces a parameter that can be used to control daylight by varying the solar shading through the surface. This aspect is also worth further exploration. Finally, the question of deployability is an interesting challenge for future work. Although intellectually satisfying and convenient for prefabrication, non-deployability may be a plus for structural performance.

References

[1] Knippers, J., and T. Helbig. (2009). Recent developments in the design of glazed grid shells. *International Journal of Space Structures* 24(2), 111–26.

[2] Schling, E. Design and construction of curved support structures with repetitive parameters. 2018. *Advances in Architectural Geometry 2018*.

[3] Mesnil, R. et al. (2015). Isogonal moulding surfaces: a family of shapes for high node congruence in free-form structures. *Automation in Construction* 59, 38–47.

[4] Douthe, C., O. Baverel, and J.-F. Caron. (2006). Form-finding of a grid shell in composite materials. *Journal of the International Association for Shell and Spatial structures* 47(1), 53–62.

[5] Kotelnikova-Weiler, N. et al. (2013). Materials for actively-bent structures. *International Journal of Space Structures* 28(3–4), 229–40.

[6] Natterer, J. et al. (2000). Roof of the main hall at EXPO 2000 in Hanover, Germany. *Structural engineering international* 10(3), 167–69.

[7] Jiang, C. et al. Curve-pleated structures. (2019). *ACM Transactions on Graphics (TOG)* 38(6), 1–13.

[8] Mesnil, R., and O. Baverel. (2023). Pseudo-geodesic gridshells. *Eng. Structures* 279, 115558.

[9] Dias, M. A., and B. Audoly. (2015). "Wunderlich, meet Kirchhoff": A general and unified description of elastic ribbons and thin rods. *Journal of Elasticity,* 119, 49–66.

[10] Lefevre, B. et al. (2017). A 4-degree-of-freedom Kirchhoff beam model for the modeling of bending–torsion couplings in active-bending structures. *Int. Journal of Space Structures* 32(2), 69–83.

[11] Wunderlich, W. (1951). Raumkurven, die pseudogeodätische Linien eines Zylinders und eines Kegels sind. *Compositio Mathematica,* 8, 169–84.

[12] Hojjat, M., E. Stavropoulou, and K.-U. Bletzinger. The vertex morphing method for node-based shape optimization. (2014). *Computer Methods in Applied Mech. and Eng.* 268, 494–513.

[13] Mesnil, R. et al. (2018). Fabrication-aware shape parametrisation for the structural optimisation of shell structures. *Engineering Structures,* 176, 569–84.

[14] Pedreschi, R. (2004). Structural innovation in pre-stressed brickwork. *Construction and Building Materials,* 18(2), 99–109.

[15] Panozzo, D., P. Block, and O. Sorkine-Hornung. (2013). Designing unreinforced masonry models. *ACM Transactions on Graphics (TOG),* 32(4) 1–12.